Theor. Appl. Climatol. 55, 3–17 (1996)

Theoretical and Applied Climatology

© Springer-Verlag 1996
Printed in Austria

State Key Laboratory of Atmospheric Sciences and Geophysical Fluid Dynamics (LASG), Chinese Academy of Sciences, Beijing, China

Research in China on Climate and its Variability

G.-X. Wu and **X.-H. Zhang**

With 18 Figures

Received October 7, 1994
Revised June 15, 1995

Summary

The research program "Dynamical Climatology and the Theory of Short-Term Climate Prediction" supported by the State Committee of Sciences and Technology is introduced. Diagnosis studies on climate variability are summarised. These include the studies on the variability of sea-surface temperature (SST) and its relationship with atmospheric anomalies, on monsoon and seasonal change, and on low-frequency atmospheric variability.

Numerical simulation and model development for climate research, particularly those activities and achievements at LASG, are reported. These include the development and simulation of atmospheric general circulation models (AGCMs), oceanic general circulation models (OGCMs), and atmosphere-ocean coupled general circulation models (CGCMs). The ongoing activities concerning the development of climate system model is also presented.

1. Introduction

The Program "Dynamical Climatology and the Theory of Short-Term Climate Prediction" was approved by the Chinese State Committee of Sciences and Technology (SCST) in 1991. This is a national program with Professor Q.-C. Zeng, the then director of LASG and of the Institute of Atmospheric Physics (IAP), as the Chief Scientist. The first five-year term is from 1991 to 1995. The main purpose of the program is, through data analysis and numerical modelling and by employing the knowledge of general circulation dynamics, geophysical fluid dynamics, and the relevant theories of math and physics, to understand the main physical processes and their variations which govern the nature of our climate system. It is organised into the following seven tasks

(1) Nature and evolution of the climate system;
(2) Persistent anomalies of atmospheric general circulation and monsoon variability;
(3) Physical processes of climate variability;
(4) Impacts of lower boundary forcing of the atmosphere on climate variability;
(5) Development of climate model and the associated mathematical problems;
(6) Numerical modelling of climate variability;
(7) Theory and method of prediction of the climate variability.

In addition to this program, some other research programs on climate variation have also been organised. These include "Climate variation and its numerical modelling" sponsored by the State Committee of Sciences and Technology, and "Prediction of disastrous climate and its impacts on agricultural yield and management of water resources" sponsored by the Chinese Academy of Sciences. Comprehensive studies under these programs have started, and remarkable progresses have been obtained. Some of the primary results from these programs are summarised in the following sections. The research on long-term climate change is included into another large

program "Study on the variation trend of our living environment in the forthcoming 20 to 50 years" sponsored by SCST and with Prof. Duzheng YE as the chief scientist. Its achievement will be reported in a separate paper, and not included here.

2. Diagnosis Study

2.1 Sea Surface Temperature (SST) Anomaly and Climate Variability

The impacts of SST on climate variability have long been studied in China (Institute of Atmospheric Physics, 1978). Recent progress occurred mainly in the research of the influences on the climate in China of the western Pacific warm pool, the equatorial Indian Ocean, the eastern equatorial Pacific, and the mid-latitude SST anomalies.

The significant impacts of the thermal feature of the western Pacific warm pool and the convective activities over the region (especially, the convective activities around the Philippines) on the intra seasonal variability of the east Asia summer monsoon circulation and rainfall have been investigated by Huang and his cooperators (1992). As shown in Fig. 1 in the year with warm SST

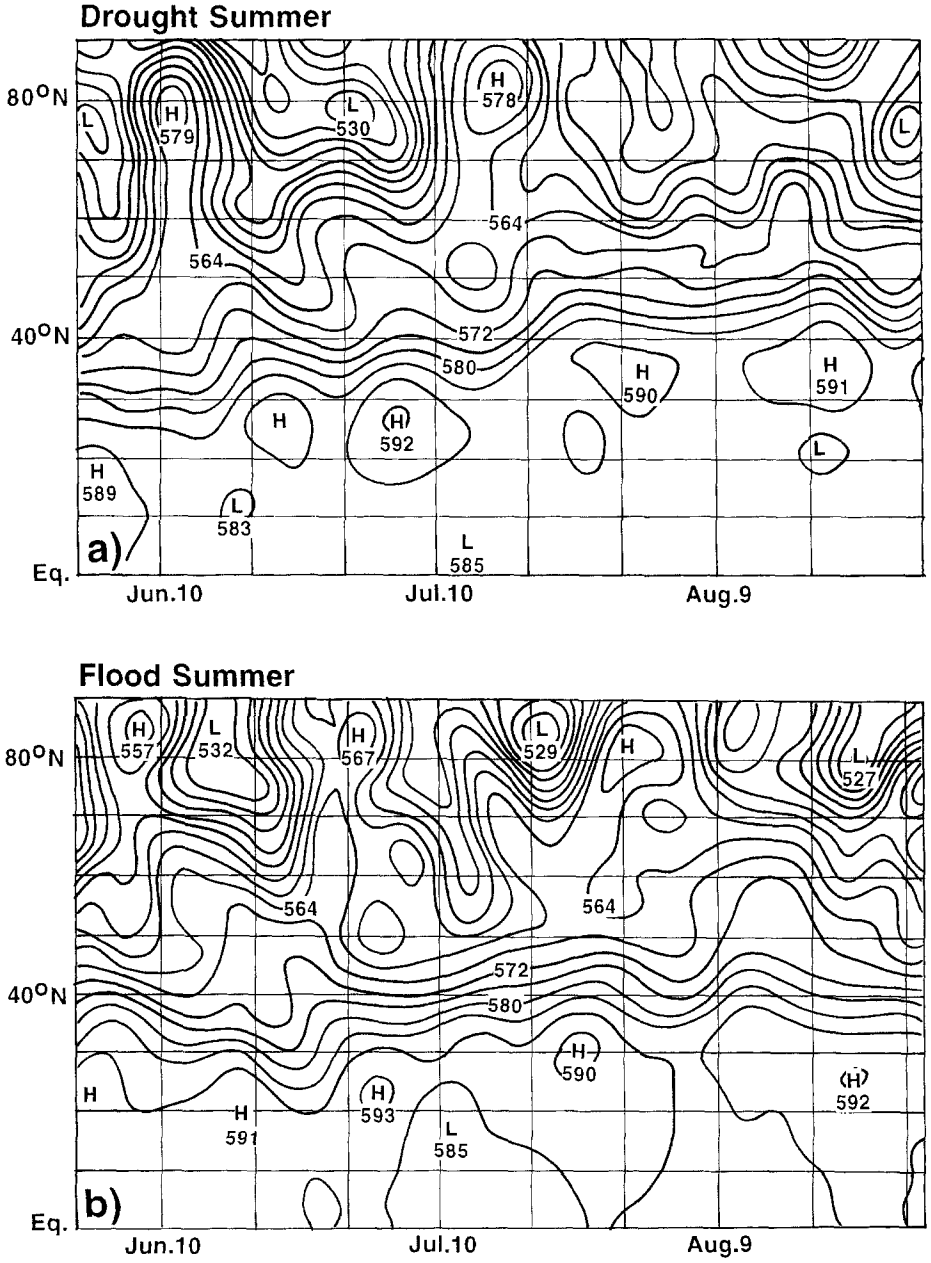

Fig. 1. Evolution of the low-pass filtered 500hPa geopotential height at 135° E. Unit in GPM. (a) 1985 when convective activity around Philippines was strong, (b) 1987 when convective activity around Philippines was weak

anomaly in the western Pacific warm pool and strong convective activities around the Philippines, the abrupt northward movement of the western Pacific subtropical high during June is obvious, and so do the seasonal abrupt change of the east Asian circulation and the northward movement of summer monsoon rain band. Whereas in the year with weak convective activities around the Philippines, the abrupt northward movement of the western Pacific subtropical high is not obvious, neither is the seasonal abrupt change of the east Asian circulation. The summer monsoon rain band is maintained over the Yangtze-Huaihe River valley, and flood used to occur there.

By analysing observed SST data, the sea temperature in the sub surface layer of the Pacific, the convective activities identified from satellite, the height fields, and the summer rainfall in China during 1978–1990, Huang et al. also found that the thermal feature in the western Pacific warm pool and the convective activities over the warm pool, especially the convective activities around the Philippines, play an important role in the interannual variability of the east Asian monsoon circulation and rainfall as well. When the SST in the western Pacific warm pool is above normal, the convective activities are strong around the Philippines in summer, then the western Pacific subtropical high shifts northward, and rainfall in the Yangtze-Huaihe River valley is below normal. On the contrary, when the SST in the western Pacific warm pool is below normal, the convective activities around the Philippines are weak in summer, then the western Pacific subtropical high shifts southward, and rainfall is above normal in the Yangtze-Huaihe River valley. In such circumstances flood usually occurs there, whereas drought usually occurs in the Yellow River valley.

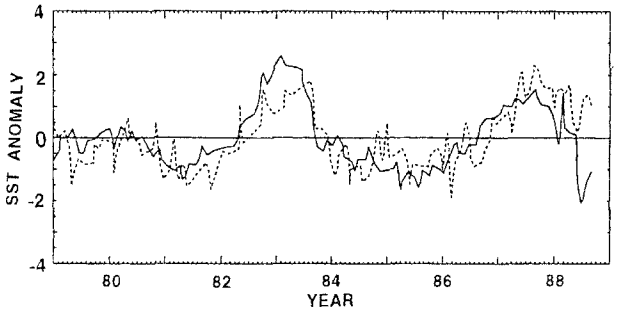

Fig. 2. Time evolutions from Jan. 1979 to Aug. 1988 of the monthly mean SST anomaly in EEP (solid curve) and CEI (dashed curve). Unit in °C

Many earlier studies have shown the significant relation between the SST anomalies in the eastern equatorial Pacific, or ENSO index, and the monsoon rainfall over China (see, for example, Fu, 1988). Using the COADS' SST data, Wu et al. (1995) found the highly significant correlation in SST between eastern equatorial Pacific (EEP) and central equatorial Indian (CEI) Ocean. Figure 2 shows the time evolutions of monthly mean SST anomaly during the period Jan. 1979 to Aug. 1988 for the EEP, and CEI region, respectively. The positive correlation between the two is pronounced. The correlation coefficient is +0.76 for a sample size of 116, far above the 99% significance level. For August SST in the EEP region, if we pick out the 3 warmest years (1982, 1983, and 1987) and the 4 coldest years (1981, 1984, 1985 and 1988), and calculate their composite means and their difference, we can then obtain the results as shown in Fig. 3. When the SST in eastern equatorial Pacific is warmer than normal, the SST in western and central equatorial Indian Ocean is also above normal.

A recent study of Lin and Yu (1993) shows that during the El Niño year, the summer rainfall along the Yangtze River can be either above or

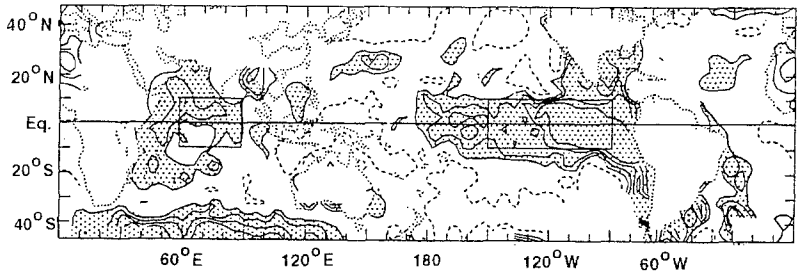

Fig. 3. The August SST difference between the EEP composite warm and cold years. Interval in 0.6 °C. Zero line has been removed

below normal, depending on the mid-latitude SST patterns. Our analysis also shows that even to the PNA pattern, mid-latitude SST pattern in the central and eastern North Pacific has stronger contribution than the equatorial SST forcing (Figures not shown).

To explain the relation between SST and monsoon rainfall, many mechanism have been proposed. These include the impacts of wave train excited by SST anomaly in the western Pacific warm pool (Huang, 1988; Nitta, 1987), the intensified Walker circulation and the meridional circulation near Philippines (Fu, 1991), and the shifting of subtropical high at 500 hPa (Huang, 1992). A simultaneous correlation analysis of Wu et al. (1992, 1995) shows that the response of atmospheric rainfall to tropical SST anomaly is a neighbourhood response. As to the mid-latitude SST, the conclusions are similar. On applying the technique of rotational principle component (RPC) analysis to the Indian and Western Pacific SST, a spatial pattern with positive SST anomaly near Kamchatka Peninsula is obtained (Fig. 4a). To calculate the correction between this SST anomaly pattern and meteorology fields, the temperature, wind and specific humidity at 850 hPa are all projected onto the eigenvector corresponding to this spatial pattern, and the results are shown respectively in Fig. 4b, 4c and 4d. The correlations are significant only in the neighbourhood of the SST anomaly region, and weakening away from the region. So does the (vq) field at 850 hPa (figures not shown). These then remind us that in response to a given SST anomaly, the vq anomaly and the relevant rainfall anomaly mainly occur in its neighbourhood region.

2.2 *Monsoon and Seasonal Variation*

Monsoon, as a prominent climate phenomena, is characterised by strong seasonal variations. Figure 5 shows the departures of January and July monthly mean wind fields from the annual mean field at the lowest model layer $\sigma = 0.991$. It was produced by using the monthly mean data averaged over a ten-year period and from the integration of a 9- layer spectral model, which is going to be presented in the following sections. In producing this figure, the 10-year annual mean has been subtracted from the 10-year January and July monthly mean for (a) and (b), respectively. This treatment can effectively remove transient systems as well as interannual variability. It can be seen from the figure that the mid-latitude semi-permanent "atmospheric activity centres", such as the boreal continental anticyclonic and oceanic

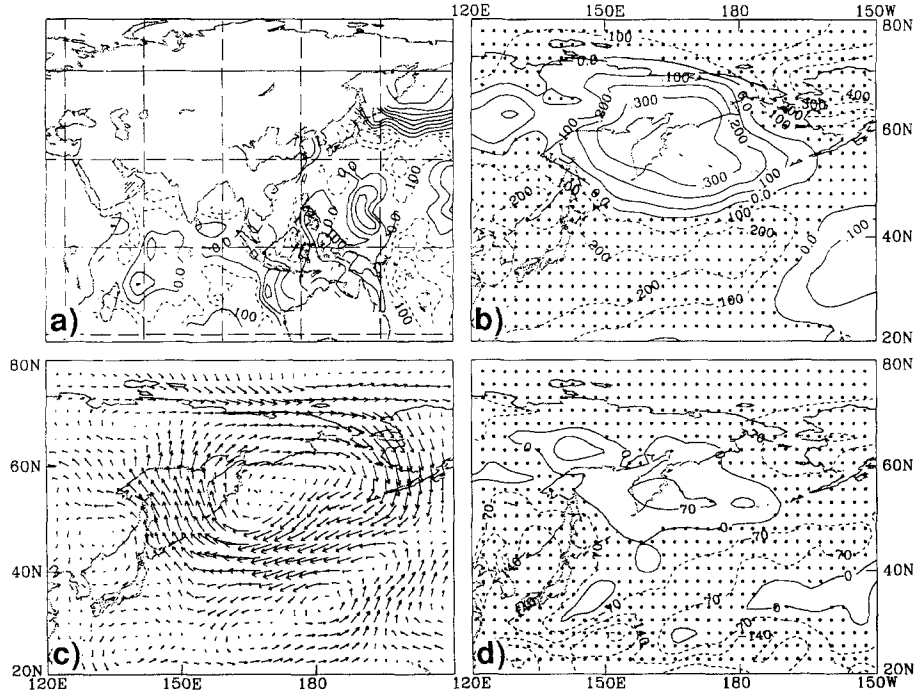

Fig. 4. One of the spatial SST pattern (a) as a component of the Indian-Western Pacific SST RPC decomposition, and the projections onto its eigenvector of the 850 hPa temperature (b), wind (c) and specific humidity (d), respectively. Data used for this study are extending from Jan. 1980 to September 1988 and all normalised

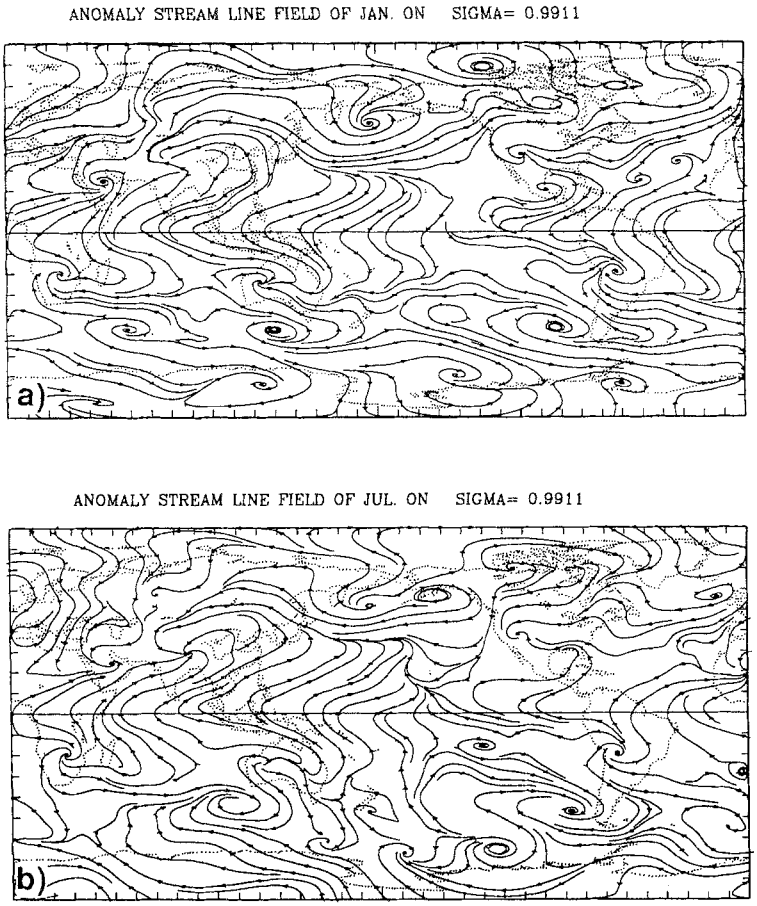

Fig. 5. The departure of the January (a) and July (b) monthly-mean winds at the $\sigma = 0.9911$ surface from their annual means. Both the monthly and annual mean data are the output of a ten-year integration of the IAP L9 R15 AGCM

cyclonic pattern in winter and their reversal in summer, and the general divergence in winter and convergence in summer in the southern hemisphere are all well defined. The seasonal changes of equatorial and tropical trade wind and monsoon systems can also be clearly specified. They are all associated with the seasonal change in land-sea thermal contrast. However, the figure shows that the monsoon system are additionally affected by the mass exchange between the two hemispheres.

In order to quantitatively depict monsoon and seasonal variation, Zeng and Zhang (1992) introduced the concept "seasonality" for a climate variable $F(\lambda, \varphi, p; t)$ as below. Let F_w and F_s be the two typical fields of F for winter and summer, respectively. $\Delta = |F_w - F_s|$ then presents the "amplitude" of seasonal change, and $\bar{F} = |F_w + F_s|/2$ approximately the annual mean of F. Seasonality δ is then defined as

$$\delta = \| \Delta \| / \| \bar{F} \|$$

where a norm $\| A \|$ is the integration of A^2 over a given area S. Figure 6 shows the seasonality δ of the 850 hPa wind speed calculated for every grid-point in the zone 40 °S–40 °N. Large seasonality can be observed in the Indian and East Asian monsoon region, Australian monsoon region, and over tropical western Pacific Ocean, as well as the regions where the mid-latitude semi-permanent "atmospheric activity centres" are located.

The timing and features of seasonal change are also affected by the underlying topography. Figure 7 shows the diagram of surface latent heat flux for the late spring and early summer of 1988 and in the latitude belt 25–37.5 °N in which the Tibetan Plateau is located. In April and May, the general feature is the westward decrease of latent heat flux from western Pacific to the Iran Plateau, with the minimum over north Africa and weak maxima over Tibet and Middle East. The western Pacific is characterised by eastward propagating synoptic system with an average duration of about 9 days. In the middle of May, the intensity

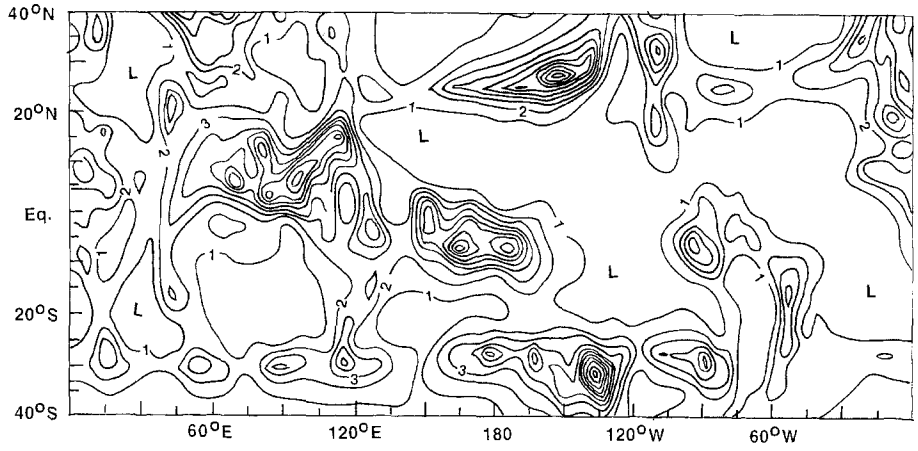

Fig. 6. Distribution of seasonality δ of the 850 hPa wind speed for 1992 (from Zeng and Zhang, 1994)

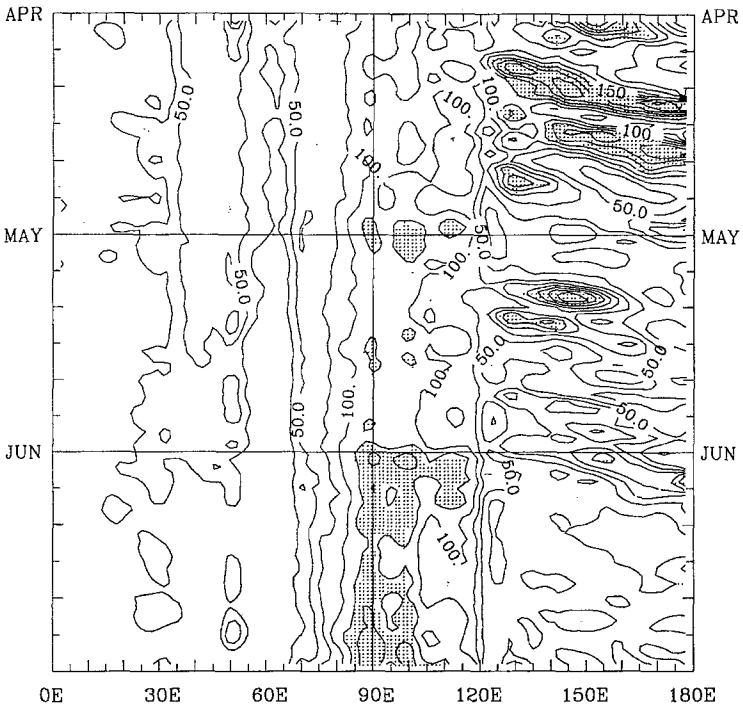

LONGITUDE–TIME CROSS SECTION OF LATENT HEAT FLUX
ON SURFACE,1988 25N–37.5N MEAN UNIT W/M/M

Fig. 7. Longitude-time cross-section of mean surface latent heat flux for the latitude zone 25–37.5° N in April, May and June of 1988

of latent heat flux over western Pacific decreases, the weak maximum in the Middle-East becomes weaker as well, and the maximum centre starts to appear over Tibet. At the beginning of June, the maximum centre of latent heat flux is at last established over Tibet, while baroclinic system ceases to develop over western Pacific. Afterwards, subtropical high dominates over the western Pacific where upward latent heat flux becomes very small, and the Middle-East weak centre disappears. Strong gradients of latent heat flux are observed at the western border of Tibet and at the eastern coast of China.

2.3 Low Frequency Variability

Earlier studies mainly based on outgoing long wave radiation (OLR) revealed the existence of intra seasonal (30–60 days) oscillation in the equatorial Pacific and south Asian monsoon regions. Using, ECMWF data, Li et al. (1991) recently calculated the distribution of perturbation kinetic energy of the 30–60 day oscillation and found that very strong kinetic energy of the low-frequency oscillation exists not only in the western equatorial Pacific and south Asian monsoon region, but also in the eastern equatorial Pacific

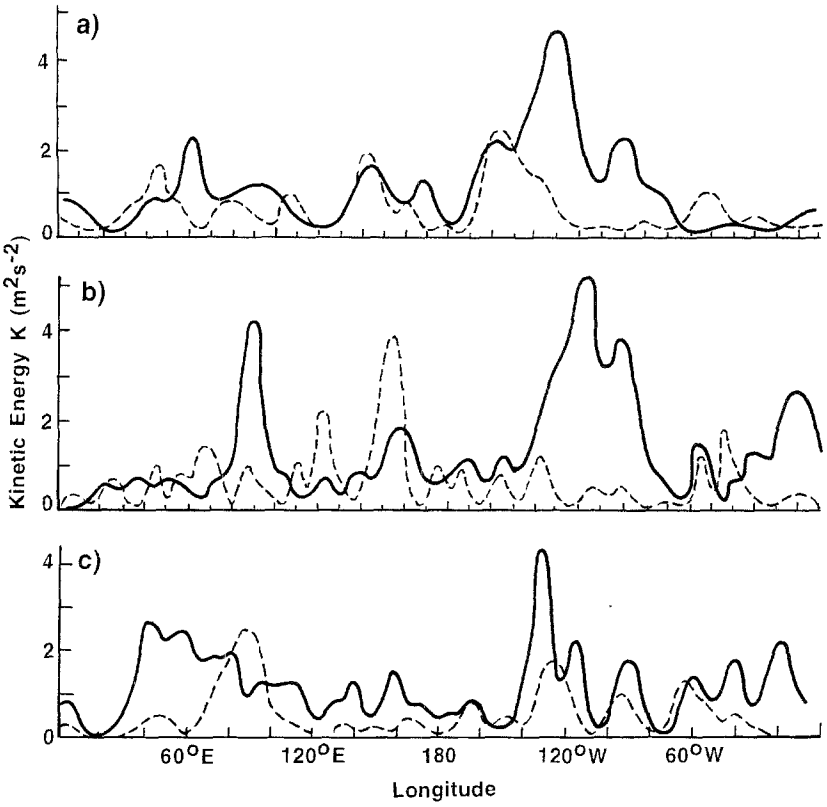

Fig. 8. Longitudinal distribution of kinetic energy of the 500 hPa 30–60 day oscillation at the equator (solid curve) and at 15° N (dashed curve). (a) January 1981; (b) January 1983; (c) July 1983 (From Li and Zhou, 1991)

(Fig. 8). They also found the relationship between tropical intra seasonal oscillation and El Niño events. Before the occurrence of El Niño event, such as in the spring and summary of 1982 and 1986, the intra seasonal oscillation is abnormally strong, especially over the western and central equatorial Pacific. It seems that such forcing effects can contribute to the generation of El Niño event (Li and Zhou, 1991). Whereas during El Niño event, interannual oscillation in the tropical atmosphere is evidently weaker.

In addition to the tropical low frequency oscillation, mid- and high-latitude oscillations were also identified. Li and his cooperators revealed that such mid-high latitude intra seasonal oscillation possesses barotropic structure in the vertical and is dominated by wave number 2 to 4 in the horizontal (figures not shown).

To understand the development of the low-frequency planetary waves typified by blocking episodes, a theory of bi-directional and single-directional cascades of kinetic energy has been developed (Wu, et al., 1995). Based on the conservation properties of gross kinetic energy K and relative potential vorticity enstrophy E for an adiabatic, frictionless, and quasi-geostrophic 2-dimensional fluid, on the introduction of spherical harmonic expansion, and on the definition of characteristic wave scale Ln ($n = s$, m, and I denote waves with smaller, medium, and larger spatial scales, respectively), the following theorem for kinetic energy conversion can be obtained:

2.3.1 Bi-Directional Transfer of Kinetic Energy

When the square of the characteristic deformation radius (L_v) of a fluid is less than, or greatly larger than, the products of the characteristic scales of any two waves involved in energy conversion, i.e., when $L_v^2 < L_q L_q$, or when $L_v^2 \gg L_p L_q$ ($p, q = s, m, l$; $p \neq q$), then the conversion of kinetic energy is bi-directional. For the latter, the amount of energy change δK subjects to the following relation

$$\delta K_l / \delta K_s \cong \frac{L_m^2/L_s^2 - 1}{1 - L_m^2/L_l^2} \quad (>1)$$

2.3.2 Single-Directional Transfer of Kinetic Energy

When the square of the characteristic deformation radius (L_v) of a fluid is between the maximum and minimum of the products of the characteristic

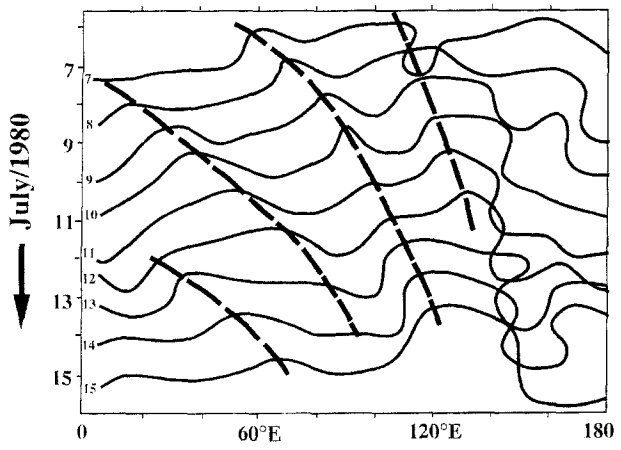

Fig. 9. Daily evolution of the 9360 gPm isoline at 300 hPa near 50° N during July 7–15, 1980. Heavy dashed line indicates ridge

scales of any two waves involved in energy conversion, ie., when $L_m L_l > L_v^2 > L_s L_m$, the conversion of kinetic energy is single-directional.

In the summer of 1980, severe and persistent drought and flooding occurred in northern and southern China, respectively. This abnormal weather is believed to be associated with continuous development and maintenance of low-frequency blocking high occurring in the northeast Asian region. In the early and middle July, there happened a complete development of blocking high. Figure 9 shows the daily evolution of the 9360 gpm contour at 300 hPa near 50 °N from 7 to 15 July, 1980. It is evident that during the period there were three synoptic systems moving eastward from Europe and west Asia to northeast Asia, and that the scale of each system when approaching the lake of Baykal became half of that in the source region ($L_m/L_s \approx 2$). Because 300 hPa is an equivalent barotropic layer, and because divergence there is small, kinetic energy transfer should subject to bi-directional cascades. In addition, the spatial scale of the time-mean blocking is about twice as large as the initial synoptic systems ($L_l/L_m = 2$, see Fig. 10). According to the above discussion, 80% of the kinetic energy of the synoptic system (K_e) should cascade to the larger-scale blocking high which possesses lower frequency (its period is longer than two weeks). To examine this transfer, a band-pass filter was used to separate high-frequency synoptic perturbations with a period of 2.5–6 days (denoted by a "prime") from other waves, and the following equation was used to calculate the transfer of kinetic energy from the larger-scale time-mean (9 days) ($\bar{K}$) to the synoptic-scale transient eddies (K_e):

$$C(\bar{K} \to K_e) = \frac{\overline{u'v'}}{a}\left[\cos\phi \frac{2}{\partial\varphi}\left(\frac{\bar{u}}{\cos\varphi}\right) + \frac{1}{\cos\varphi}\frac{\partial\bar{v}}{\partial\lambda}\right] - \frac{1}{a}\left[\overline{(v')^2} - \overline{(u'^2)}\right]\left[\frac{1}{\cos\varphi}\frac{\partial\bar{u}}{\partial\lambda} - tg\varphi\cdot\bar{v}\right].$$

and its spatial distribution is demonstrated in Fig. 10. It becomes apparent that along the time-mean westerly jet and over the blocking region, there does exist energy transfer from synoptic eddies (K_e) to the larger-scale time-mean systems. Combining Figs. 9 and 10, we may conclude that when those synoptic eddies propagated eastwards from Europe, their kinetic energy experienced bi- directional cascades. While a small portion of its energy is transferred downscally, its major part is upscale-cascaded to

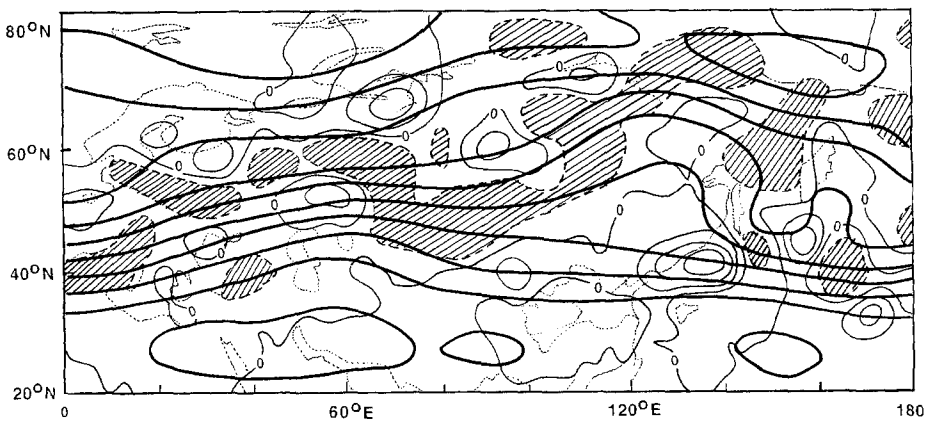

Fig. 10. Spatial distribution of the conversion of kinetic energy from time-mean larger-scale ($\bar{K}$) to transient synoptic-scale (K_e), i.e., $C(\bar{K} \to K_e)$, at 300 hPa in the period July 7–15, 1980. Solid and dashed curves denote positive and negative values, respectively. Interval in $1 \times 10^{-4}\,m^2\,s^{-3}$. Heavy solid lines show the time-mean geopotential contours. Hatched region denotes where C is less than $(-1 \times 10^{-4}\,m^2\,s^{-3})$

larger systems, and resulting the formation of the blocking.

This study reminds us that when we try to predict the northeast Asian blocking, which has strong impacts on the persistent anomalous weather in China in summer, attention should be paid to the development of baroclinic systems over Europe and western Asia.

3. Model Development and Numerical Simulation

Numerous models have been developed in China to simulate climate variability. As LASG has been taking the most substantial responsibilities in model development for the study of dynamical climatology, here we will concentrate on the progresses occurring at LASG. The 2-layer IAP AGCM, and the IAP CGCM with 2-layer for the atmosphere and 4-layer for the ocean, which were developed in the middle 1980', are still being used in China, and the details of these models and their performances can be referred to Zeng et al. (1987, 1989), Zhang and Liang (1989) and Zhang et al. (1992). In this section we will present the latest achievements in the field during the last three years.

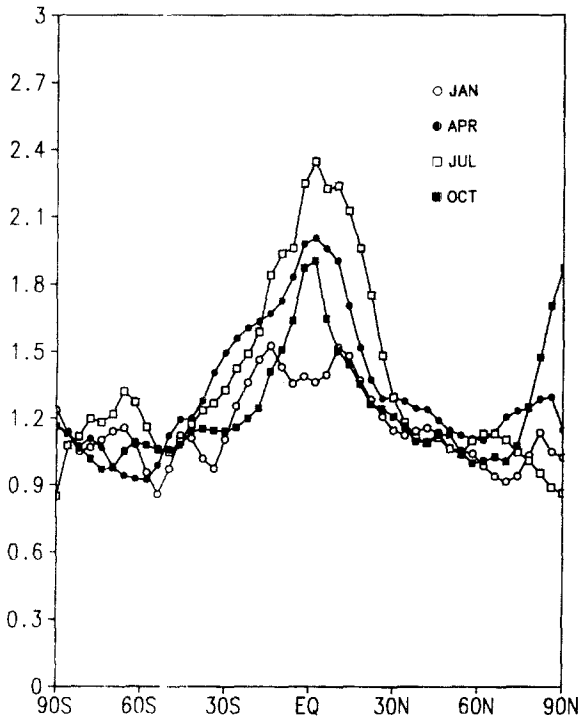

Fig. 11. The latitude distribution of the zonally averaged ratio between IAP CGCM and IAP AGCM model results of the standard deviation of monthly mean sea-level-pressure from its climate means (By courtesy of Yu and Guo, 1994)

The 2-layer IAP AGCM has satisfactorily reproduced many aspects of the mean climate (Zeng et al., 1990; Xue, 1992). In a model integration of 25 years with climate mean SST as lower boundary forcing, Xue found that the southern oscillation does not exist, and the interannual climate variability is weak. The standard deviation of monthly mean sea level pressure (SLP) from its climate average is only half of that in the observations. On analysing a 40-year integration output of the IAP CGCM, Yu and Guo (1994) successfully identified the southern oscillation pattern (figures not shown), and found that the standard deviation of the monthly mean SLP in the tropics is about double compared to the AGCM results (Fig. 11), much closer to the observation. This means that a substantial part of the climate interannual variability in the tropics is associated with the air-sea interactions.

3.1 Atmospheric General Circulation Model (AGCM)

3.1.1 IAP 9-Layer Gridpoint (IAP L9G) AGCM

Within the framework of cooperation research between Chinese Academy of Sciences and the Department of Energy of the United States on the climate impacts of increasing CO_2, in the period of 1987–1991, a nine-layer gridpoint AGCM named as IAP/SUNY L9G was developed by the common efforts of X.-Z. Liang, X.-H. Zhang, Q.-C. Zeng and R. D. Cess (Liang, 1991[1]; Zhang, 1990). This model possesses some unique features in the development of dynamic framework, in computation scheme, and in parameterizations of physical processes, and showed its ability in climate modelling. In 1992, Bi and Zeng used the climate monthly-mean data of sea surface temperature (SST) and sea ice (SI) as the lower boundary condition and integrated the model, with some improvements, for 5 years. The results show that the mean January and July climate were reasonably simulated.

[1] Liang, Xingzhong, 1991: A brief description of the IAP/SUNY 9-level AGCM. Personal communication.

3.1.2 IAP 9-Layer Spectral (IAP L9R15) AGCM

Since the end of 1991, we have introduced a nine-layer spectral model which is rhomboidal truncated at zonal wave number 15, and engaged in a series of work for its reformation and development. The model was originally transferred by Lin (1991) from the version of Simmonds (1985). It suffered from serious global cooling and, particularly, from serious negative orography effects. Around steep mountains, such as Tibetan plateau, Rockies, Andes, and Antarctica, many false systems and systematic errors were found. Our efforts during the last 2 years mainly include the introduction of more realistic external forcing to the model atmosphere, and the reformation of its dynamic framework by deducting "a standard atmosphere" from the set of governing equation (Phillips, 1973; Zeng, 1963). These make the model perform much better. By using the "AMIP" SST and SI Dataset from January 1979 to December 1988, the model has been integrated for the ten-year period. Figure 12 shows the simulated sea-surface pressure for January (a) and July (b), respectively. The Aleutian and Icelandic low, and Eurasian and North American high in the boreal

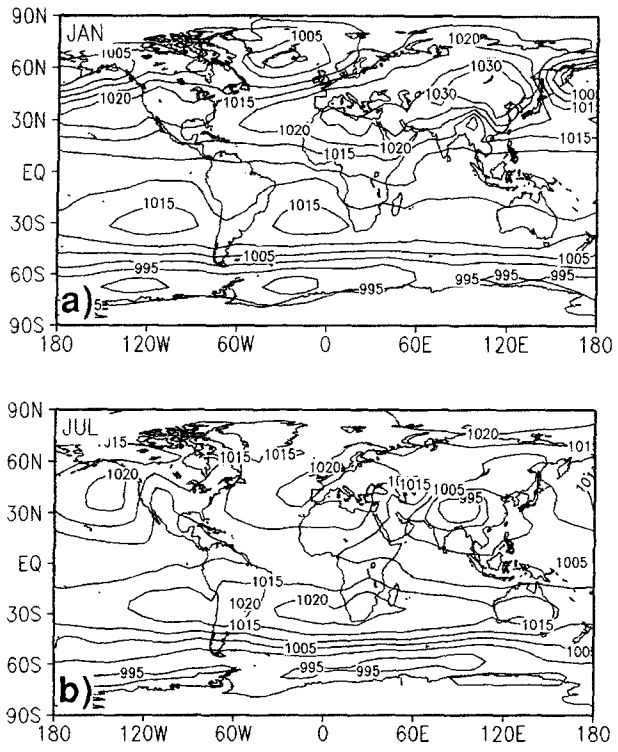

Fig. 12. Distribution of monthly mean sea-level pressure (hPa) for January (a), and July (b) simulated from the IAP L9R15 spectral model for the period 1979–1988

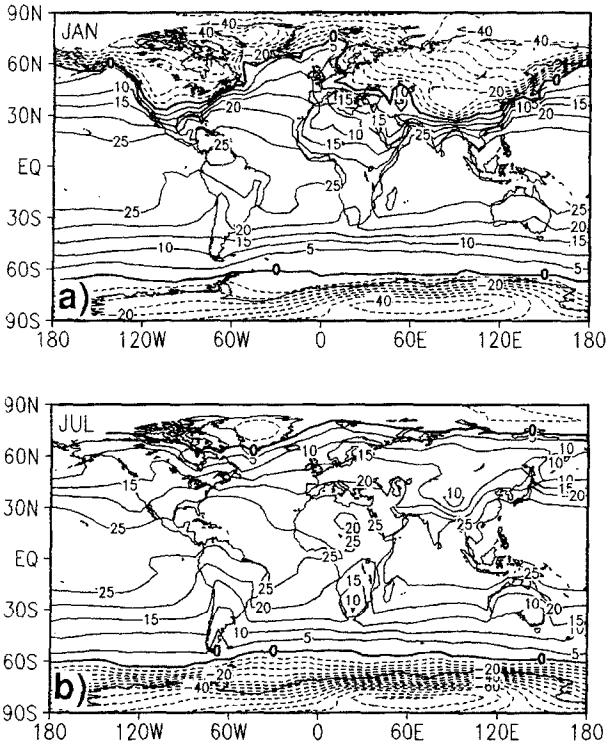

Fig. 13. Distribution of monthly mean surface air-temperature (°C) for January (a), and July (b) simulated from the IAP L9R15 spectral model for the period 1979–1988

winter, the continental low and oceanic high in the boreal summer, and the permanent oceanic high and the pronounced "roaring forties" in the southern hemisphere are all simulated remarkably well. The simulated surface temperature (Fig. 13) are also in very good correspondence with observations. In Figs. 14 and 15 are shown the comparison of precipitation between the time-mean observation (a) and simulation (b) for Dec., Jan., and Feb. (DJF), and for Jun., Jul., and Aug. (JJA), respectively. During DJF (Fig. 14), the dryness over the boreal continent, the ITCZs, and the heavy precipitation centres over southern American and the southeast of Africa are reproduced. During JJA (Fig. 15), the observed three centres of tropical rainfall are also represented in the model. The monsoon precipitation along the monsoon trough is particularly well reproduced both in location and in intensity.

3.2 Ocean General Circulation Model (OGCM)

3.2.1 High Resolution Pacific OGCM (POGCM)

Based upon the original 4-layer IAP OGCM, R.-H, Zhang et al. (1994) developed a 14-layer high resolution (1° lon. × 2° lat.) OGCM for the

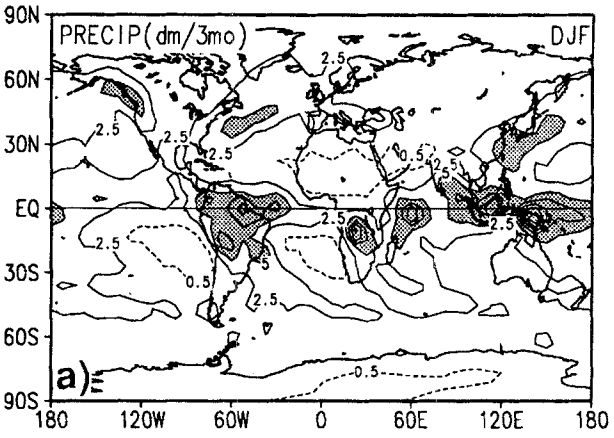

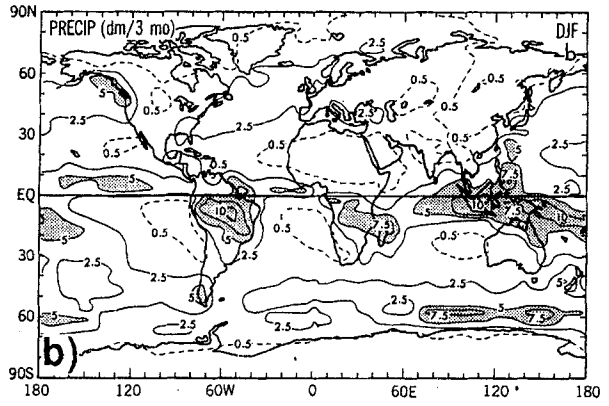

Fig. 14. Distribution of seasonal mean precipitation (dm/3mo) for December, January, and February (DJF). (a) Simulated for the period 1979–1988; (b) Observed from Peixoto and Oort (1992)

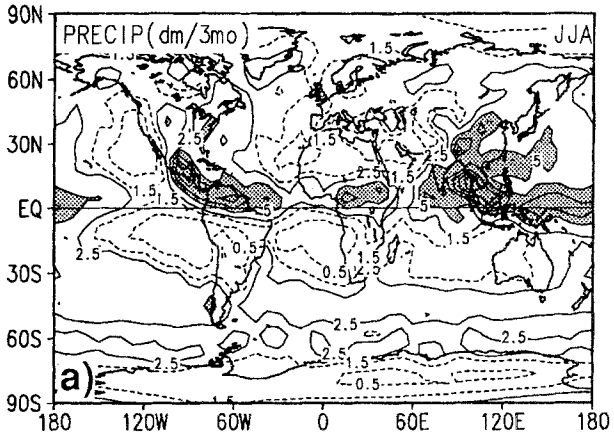

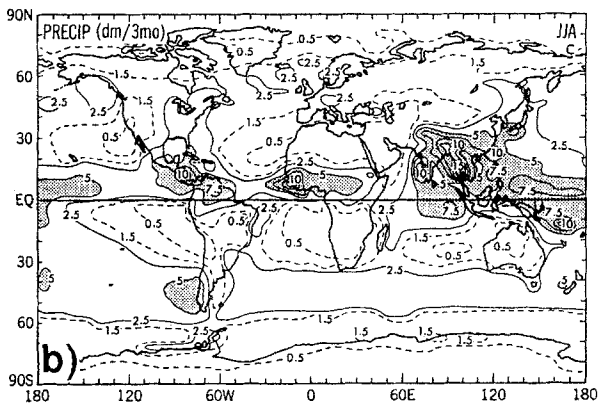

Fig. 15. As in Fig. 16, except for June, July, and August (JJA)

tropical Pacific area. Salinity was predicted. Parameterization scheme for vertical diffusion and that for convective adjustment were considered as functions of current shear and stratification stability. This model has been integrated for a period of several years and for some simulation studies. With the forcing of the observed wind stress, heat flux, and fresh-water flux at sea-surface, the model has successfully simulated the sea-level elevation, the mid-equator trough and ridge, the north equatorial counter-current, the sub-surface thermocline, the equatorial undercurrent, and some meso-scale eddies. The eastward propagation of warm SST at the equator during the El Niño event of 1986–1987, and the cooling of SST over the equatorial Pacific in the La Niña year 1988 have also been reproduced in the model (figures not shown).

3.2.2 The 20-Layer Global OGCM

In order to improve the simulation of thermohaline circulation in the ocean and sea-ice at high-latitudes, a 20-layer global OGCM has been developed at LASG by X.-H. Zhang and his cooperators (1993). Compared to the original 4-layer OGCM, considerable improvements in both dynamical and physical designs have been added in the new model. These include the followings.

* The standard stratifications of temperature, salinity, density and pressure are considered to be functions of both depth and latitude, rather than depth alone, so that the formation of thermohaline circulation can be speeded up.
* The Mesinger's η-vertical coordinate which was used by R.-C. Yu (1989) for a regional NWP model is adopted. Therefore the complex orography at sea base can be presented more adequately than in the σ-coordinate

system. The maximum and minimum depth of the model is now 5000 m and 50 m respectively.

* The formation and melting of sea ice have been included by referring to the work of Semtner (1976) and Parkinson and Washington (1979). The ice-ocean interaction has also been simply considered.
* A splitting scheme in temporal integration for calculating barotropic mode, baroclinic mode, and thermohaline processes has been adopted. To make calculation economic and stable, the schemes of Killworth (1989) and Mellor (1993) were used to deal with the "separation" and "interaction" between barotropic and baroclinic modes, and the Asselin time filter (Asselin, 1972) was adopted.
* In addition to the explicit diffusion, an "implicit" diffusion induced by using "upwind finite-difference" scheme in treating temperature and salinity diffusion (see Maier-Reimer et al., 1991) was also introduced.

By using the observed monthly mean wind stress (Hellerman et al., 1983), SST, pressure, water mixing ratio, wind, short wave radiation and cloudiness (Esbensen et al., 1981), and surface salinity (Levitus, 1982), the model has been integrated for more than 700 years. The results show that this model is capable of simulating SST, salinity, sea current, sea-level, and up welling and down welling, etc. More encouragingly, it produces reasonable thermohaline circulation. In Fig. 16 and Fig. 17 are shown the annual mean

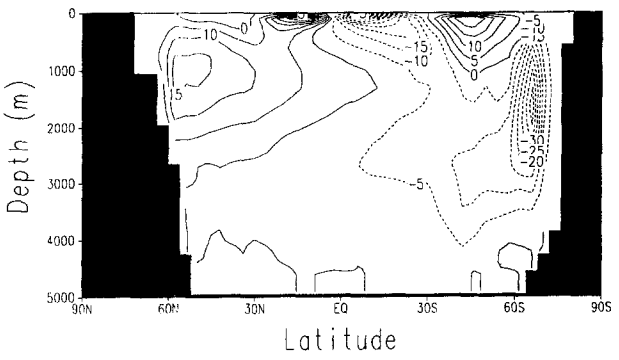

Fig. 16. Zonal mean meridional streamfunction of the thermohaline circulation of the 700th model year in the integration of IAP L20 OGCM. Units in Sv. ($10^6\ m^3\ s^{-1}$)

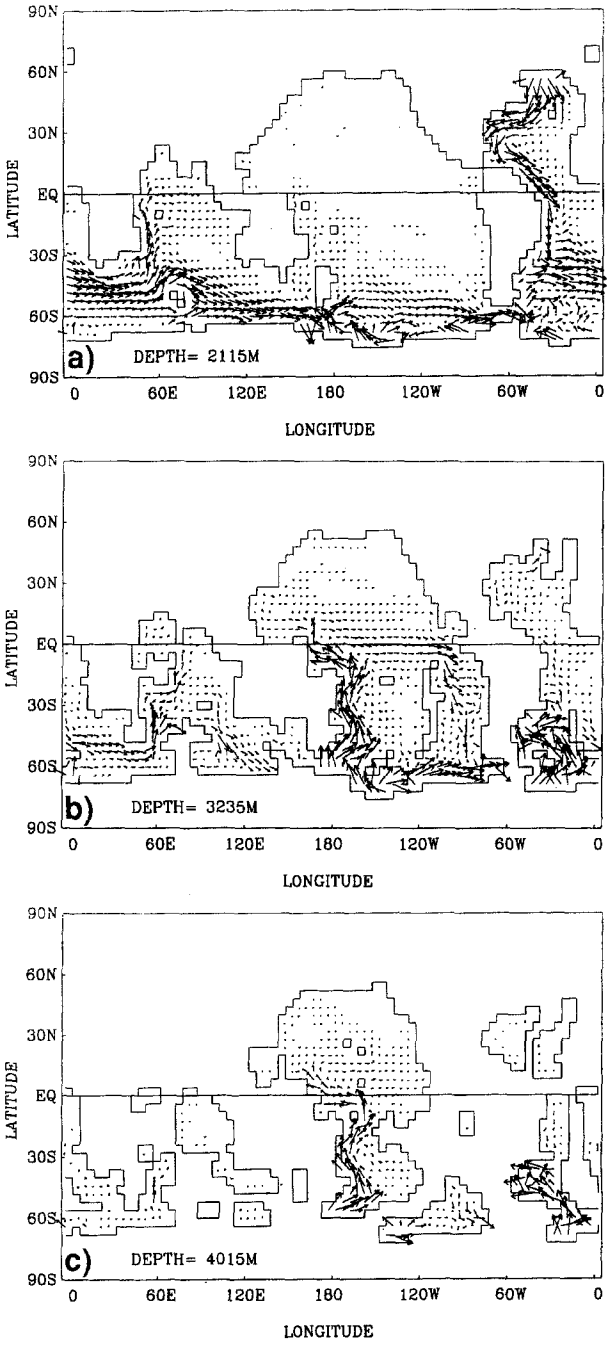

Fig. 17. Distribution of the thermohaline current of the 700th model year in the integration of IAP L20 OGCM. (a) At 2115m; (b) at 3235 m; (c) at 4015m

results of the 700th year for mean meridional streamfunction, and for the flow fields at the depth of 2000 m, 3000 m, and 4000 m, respectively. It can be seen that the north Atlantic deep water (NADW) at 2 km and the Antarctic bottom water (AABW) at 3 and 4 km are well represented in the model.

3.3 Global Atmosphere-Ocean Coupled GCM (CGCM)

In order to diminish the "climate drift" in a coupled atmosphere-ocean GCM, Zhang and his cooperators (1992) developed a special coupling scheme named as "prediction-correction monthly mean flux anomaly coupling scheme". With this scheme, a CGCM consisting of the IAP two-layer AGCM and four-layer OGCM was integrated for forty years without serious model's drift. More than this, the CGCM is capable to simulate significant interannual climatic variability in the tropical Pacific region. Figure 18 is the time-longitude plot of the monthly mean SST anomalies in the equatorial Pacific for the model' years from 7th to 36th. It exhibits clearly the westward phase propagation of the SST anomalies with the maximum of above 1 °C during this thirty-year period, which is quite similar to the simulation of Meehl (1990).

The aforementioned coupling scheme has been generalised to include the air-sea-sea ice interaction. Recently, the twenty-layer OGCM was coupled with the two-layer AGCM by using the generalised scheme to simulate the time-dependent response of the coupled system to a gradually increasing atmospheric CO_2 concentration. By now, the new coupled model has been successfully integrated for more than 100 years for its control run at LMD/CNRS by K.-M. Chen in cooperation with French scientists (Chen, personal communication).

3.4 On going Activities

Most of the model development activities at LASG are organised in accordance with the requirement of the study of our climate system. For this purpose, models for individual climate sub systems, and schemes for presenting interactions between different sub systems are both needed.

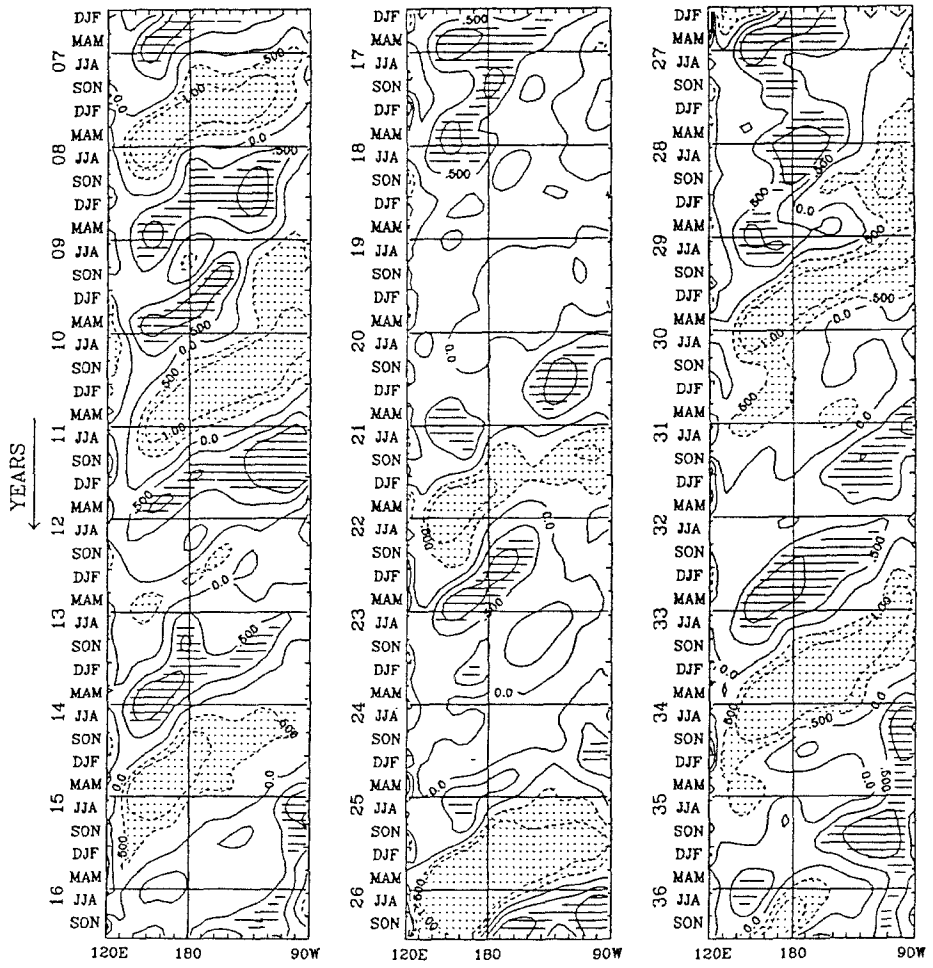

Fig. 18. Time-longitude plot of the monthly mean SST anomalies in the equatorial Pacific for the model year 7–36 in the integration of IAP CGCM. Units in °C

In addition to the development of AGCM, OGCM, and A-O CGCM described in the above sections, a group of scientists headed by S.-F. Sun and J. J. Ji is working on the development of a multi-layer land-surface model, and a simple biosphere model, while another group headed by X.-H. Zhang is developing a sea-ice model for polar cap regions. A modified Wang-Shi scheme proposed by G.-Y. Shi is being mounded to the L9R15 AGCM to present the radiation impacts of clouds and atmospheric consistents.

We hope that through these efforts, we will be able to model the chemical processes in our climate system in the near future.

4. Summary

When invited to prepare a key presentation on climate variability research in China for the Vth International Summer Colloquium of LASG, which is held every other year, and for the Session 3 of the International Symposium on Global Change in Asia and the Pacific Region (GCAP), held in Beijing on August 8 to 10, 1994 and chaired by Professor Duzheng Ye, we were facing great difficulties. As climate and its variability have been becoming popular subjects, relevant papers, reports, and even conferences or symposiums come out one after another. It is then impossible to present all research activities and results for such a big country by only a simple paper. However, there were five sessions in GCAP. In addition to "climate variability", other subjects, such as the "past global change", the "global change impact and terrestrial ecosystem", the "biogeochemical cycle and greenhouse gases", and the "earth observation for global change", have been framed to other sessions. We were then able to focus on a relatively narrower scene. Even so, what we have summarised in this paper is only parts of the results obtained from the program Dynamical Climatology and the Theory of Short-Term Climate Prediction and at LASG. Therefore, the results and activities reported here should be regarded as one window through which our colleagues can pear at the whole activities in China.

Comprehensive activities in the study of climate variability in China are also organised to cover some frontier fields. New national Programs are being planned and will soon be implemented. These include the Chinese Global Energy and Water Experiment (GEWEX), the Middle Atmosphere Research, the South China Sea Monsoon Experiment, and the Physical Processes of the Land-Air System of the Tibetan Plateau and Global Climate, etc. There is no doubt that in the near future China will take a much more active part in the research of climate variability in the world community of sciences and development.

Acknowledgment

We would like to thank Prof. Dirmhirn, the former Chief Editor of T.A.C, for her great efforts in stimulating, and supporting the publication of this report. Thanks are also to Ms. Xuan Wang for typing the manuscript.

References

Asselin, R., 1972: Frequency filter for time integrations. *Mon. Wea. Rev.*, **100**(6), 487–490.

Esbensen, S. K., Kushinir, Y., 1981: Heat budget of the global ocean: estimate from surface marine observations, Report No. 29, Climate Research Institute, Oregon State Univ., Corvallis, Oregon, 271pp.

Fu, C., 1991: Processes in ocean and climate variability. In: Ye, D., et al. (eds.) *Contemporary Climate Research.* Beijing: Chinese Meteor. Press, pp. 211–235.

Hellerman, S., Rosenstein, M., 1983: Normal monthly wind stress data over the world ocean with error estimates. *J. Phys. Oceanogr.*, **13**, 1093–1104.

Huang, R., Li, W., 1988: Influence of the heat-source anomaly over the western tropical Pacific on the subtropical high over east Asia during summer and its physical mechanism. *Chinese J. Atmos. Sci.* (Special Issue), pp. 107–116.

Huang, R., Sun, F. 1992: Impacts of the tropical western Pacific on the east Asian monsoon. *J. Meteor. Soc. Japan*, **70**, 243–256.

Institute of Atmospheric Physics, 1978: *Air-sea Interaction and long-range Forecasts of Drought and Flooding.* Beijing: Chinese Science Press, 129pp, in Chinese.

Killworth, P. D., Staniforth, D. J., Webb, D. J., Paterson, S. M., 1989: A free-surface Bryan-Cox-Semtner model, Report No. 270 (Reprinted 1993), Institute of Oceanographic Sciences, Deacon Laboratory, 87pp.

Levitus, S., 1982: Climatological Atlas of the World Ocean, NOAA Professional Paper 13, US. Governmental Printing Office, Washington, D.C., 173pp.

Li, C., 1991: *Atmospheric low Frequency Oscillation.* Chinese Sciences Press, Beijing: pp. 207.

Li, C., Zhou, Y., 1991: An observational study of the 30–50 day atmospheric oscillations. Part II: Temporal evolution and hemispheric interaction across the equator. *Advances Atmos. Sci.*, **8**, 399–406.

Lin, X., Yu, S., 1993: El Niño and rainfall during the flood season (June-August) in China. *ACTA Meteor. Sinica*, **51**, 434–441.

Lin, Y., 1991: General circulation experiments at Guangzhou

Institute of Tropical Oceanography and Meteorology. 14 pp.

Maier-Reimer, E. U., Mikolajewicz, U., Hasselmann, K., 1991: On the sensitivity of the global ocean circulation to changes in the surface heat flux forcing, Report No. 68, Max-Planck-Institut Meteorologie, Hamburg, July 1991, 67pp.

Meehl, G. A., 1990: Seasonal cycle forcing of El Niño/Southern Oscillation in a global coupled ocean-atmosphere GCM. *J. Climate,* **3**, 72–98.

Mellor, G. L., 1993: *User's Guide for a Three-dimensional, Primitive Equation, Numerical Ocean Model.* Princeton, New Jersey, USA: Princeton University, Princeton, 35pp.

Nitta, Ts., 1987: Convective activities in the tropical western Pacific and their impact on the northern hemisphere summer circulation. *J. Meteor. Soc. Japan,* **64**, 373–390.

Parkinson, C. L., Washington, W. M., 1979: A large-scale numerical model of sea ice. *J. Geophys Res.,* **84**, 311–337.

Peixoto, J. P., Oort, A., 1992: *Physics of Climate.* New York, USA: AIP press, 520pp.

Phillips, N. A., 1973: Principles of large scale numerical weather prediction. In: Morel, P. (ed.) *Dynamic Meteorology.* Dordrecht-Holland: D. Reidel Publishing, pp 1–96.

Schlesinger, M. E., Gates, W. L., 1980: The January and July performance of the OSU two-level atmospheric general circulation model. *J. Atmos. Sci.,* **37**, 1914–1943.

Semtner, A. J. Jr., 1976: A model for the thermodynamic growth of sea ice in numerical investigations of climate. *J. Phys. Oceanogr.,* **20**, 600–609

Simmonds, I., 1985: Analysis of the "spinning" of a global circulation model. *J. Geophys. Res.,* **90**, 5637–5660.

Wu, G., 1995: Bi-directional and single-directional cascade of kinetic energy of the atmosphere. *Chinese J. Atmos. Sci.,* **19**, 52–62.

Wu, G., Huangzhu, Liu, 1992: Atmospheric precipitation in response to equatorial and tropical sea surface temperature anomalies. *J. Atoms. Sci.,* **49**, 2236–2255.

Wu, G., Sun, F., Wang, J., Wang, X., 1995: Neighbourhood response of atmospheric precipitation to tropical sea-surface temperature anomalies. *Chinese J. Atmos. Sci.,* **19**, 664–676.

Xue, F., 1992: The diagnostic analyses and validation of climate simulation of IAP AGCM. Doctoral Thesis of IAP/CAS (in Chinese).

Yu, R., 1989: Design of the limited area numerical weather prediction model with step mountains. *Scientia Atmospherica Sinica,* **13**(2), 139–149.

Yu, Y., Guo, Y., 1994: The interannual variability of climate in a coupled ocean-atmosphere model. *Advance Atmos. Sci.* (in press).

Zeng, Q., 1963: Characteristic parameter and dynamical equation of atmospheric motions. *Acta Meteor. Sinica,* **33**, 472–483 (in Chinese).

Zeng, Q., Yuan, C., Zhang, X., Liang, X., Bao, N., Wang, W., 1990: IAP AGCM and its application to the climate studies, pp. 303–330, The Third International Summer Colloquium of LASG on Climate Change, Dynamics and Modelling, Ed. Zeng et al., 390pp.

Zeng, Q., Yuan, C., Zhang, X., Liang, X., Bao, N., 1987: A global gridpoint general circulation model. Proceedings of the WMO/IUGG NWP Symposium, Tokyo, 4–8 August, 1996. *J. Meteor. Soc. Japan,* (Special Volume), 121–142.

Zeng, Q., Zhang, B., 1992: On the seasons of atmospheric general circulation and their abrupt changes – Part I: general concept and method. *Chinese J. Atmos. Sci.,* **16**, 329–336.

Zeng, Q., Zhang, X., Liang, X., Yuan, C., Chen, S.-F., 1989: Document of IAP Two-Level AGCM. TR 044, DOE/ER/60314, -H1, U.S. DOE., p. 383.

Zhang, R., 1994: Simulation of the 1986–1987 El Niño and 1988 La Niña events with a free surface tropical Pacific Ocean general circulation model. *J. Geophys. Res.,* **99**, C4, 7743–7759.

Zhang, X., Liang, X., 1989: A numerical would ocean general circulation model. *Adv. Atmos. Sci.,* **6**, 44–61.

Zhang, X., 1990: Dynamical framework of IAP nine-level atmospheric general circulation model. *Adv. Atmos. Sci.,* **7**, 67–77.

Zhang, X., Bao, N., Yu, R., Wang, W., 1992: Coupling scheme experiments based on an atmospheric and oceanic GCM. *Chinese J. Atmos. Sci.,* **16**/2, 129–144.

Zhang, X., Chen, K., Jin, X., Lin, W., Yu, Y., 1993: A twenty-layer oceanic general circulation model, Report at the 1993 Annual Conference of LASG, Beijing Jan. 10–11, 1994.

Authors' address: G. Wu and X. Zhang, State Key Laboratory of Atmospheric Sciences and Geophysical Fluid Dynamics (LASG), Chinese Academy of Sciences, Beijing, 100080 China.